analytical chemistry

Article

pubs.acs.org/ac

Size-Dependent Programming of the Dynamic Range of Graphene Oxide–DNA Interaction-Based Ion Sensors

Huan Zhang,[†,∥] Sisi Jia,[†,∥] Min Lv,[†] Jiye Shi,[‡] Xiaolei Zuo,[†] Shao Su,[§] Lianhui Wang,[§] Wei Huang,[§] Chunhai Fan,[†] and Qing Huang*[,†]

[†]Division of Physical Biology & Bioimaging Center, Shanghai Synchrotron Radiation Facility, Shanghai Institute of Applied Physics, Chinese Academy of Sciences, Shanghai, China

[‡]UCB Pharma, Slough SL1 3WE, U.K.

[§]Key Laboratory for Organic Electronics & Information Displays (KLOEID) and Institute of Advanced Materials (IAM), Nanjing University of Posts & Telecommunications, Nanjing, China

Supporting Information

ABSTRACT: Graphene oxide (GO) is widely used in biosensors and bioimaging because of its high quenching efficiency, facile chemical conjugation, unique amphiphile property, and low cost for preparation. However, the nanometer size effect of GO on GO–DNA interaction has long been ignored and remains unknown. Here we examined the nanometer size effect of GO on GO–DNA interactions. We concluded that GO of ∼200 nm (lateral nanometer size) possessed the highest fluorescence quenching efficiency whereas GO of ∼40 nm demonstrated much weaker ability to quench the fluorescence. We employed the nanometer size effect of GO to program the dynamic ranges and sensitivity of mercury sensors. Three dynamic ranges (1 to 40 nM, 1 to 15 nM, and 0.1 to 5 nM) were obtained with this size modulation. The sensitivity (slope of titration curve) was programmed from 15.3 ± 1.27 nM^{-1} to 106.2 ± 3.96 nM^{-1}.

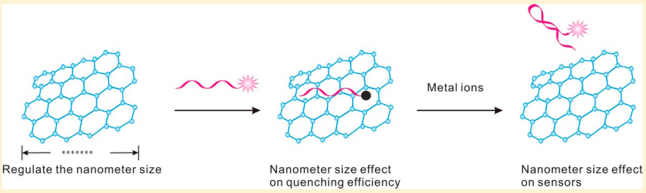

Nanometer size is critically important for nanomaterials to possess excellent properties.[1−3] The ability to tune the nanometer size of nanomaterials provides powerful tools to tailor their optical, electronic, magnetic, and biological properties.[3−12] Hence, nanomaterials with tunable properties have been extensively investigated and are widely used in bioimaging, diagnosis, and therapy.[13−17]

Graphene oxide (GO) is a two-dimensional carbon material that has attracted intensive research interest in recent years.[18−20] Its wide applications in electronics, optics, biology, and diagnostics have been explored.[19,21] Particularly, GO is widely used in biosensors and bioimaging because of its high fluorescence quenching efficiency, facile chemical conjugation, unique amphiphile property, and low cost for preparation.[18,21] Varieties of fluorescent biosensors have been successfully developed for the detection of DNA, proteins, small molecules, and ions.[22−41] In these designs, high fluorescence quenching efficiency of GO as well as its high differentiation ability for different structures of bioprobes are employed to achieve simple, sensitive, and specific detections. Usually, the binding forces between GO and single-stranded DNA (ssDNA) (that include hydrophobic force and $\pi-\pi$ stacking interaction) are much stronger than that between GO and double-stranded DNA (or folded DNA).[24,34]

Despite what has been achieved so far, the nanometer size effect of GO on DNA–GO interaction is not well understood. Here, we investigated the nanometer size effect of GO on DNA–GO interaction by employing GO with three different nanometer sizes and fluorophore-modified oligonucleotides. By comparing the fluorescence quenching efficiency, we concluded that GO with nanometer size of ∼200 nm possesses quenching efficiency higher than that with nanometer size of >500 nm and ∼40 nm. On the basis of these interesting findings, we regulated the dynamic ranges of an ion sensor for Hg^{2+}. We obtained tunable dynamic ranges by regulating the nanometer size of GO.

RESULTS AND DISCUSSION

To prepare GO with different nanometer sizes, we employed Hummers's method[42] for GO1 (average nanometer size is >500 nm) and repeated oxidation for GO2 (average nanometer size is ∼200 nm) and GO3 (average nanometer size is ∼40 nm) (Figure 2). The repeated oxidation was an efficient cutting technique and employed to prepare the relatively small GO2 and GO3. Precise control of the GO size remains challenging. Therefore, the size of GO is distributed in a range of nanometers. We characterized the GOs by AFM (atomic force microscopy) and found that the thicknesses of GO1, GO2, and GO3 are all ∼1.1 nm, which demonstrated the characteristic of a fully exfoliated GO sheet and was similar to previous reports.[24] As we expected, their average lateral

Received: February 14, 2014
Accepted: March 18, 2014
Published: March 18, 2014

   dx.doi.org/10.1021/ac500627r | *Anal. Chem.* 2014, 86, 4047−4051

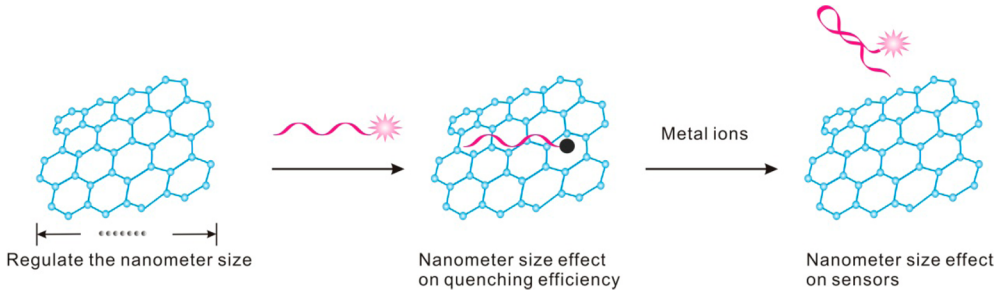

Figure 1. The nanometer size of GO can be regulated through chemical oxidation. We obtained GO with three different nanometer sizes (their size ranges from tens to hundreds of nanometers). We investigated the different quenching efficiencies of the three types of GO, which indicated that the quenching efficiency is nanometer size dependent. Then, on the basis of these findings, we designed sensors for mercury ions with tunable dynamic ranges.

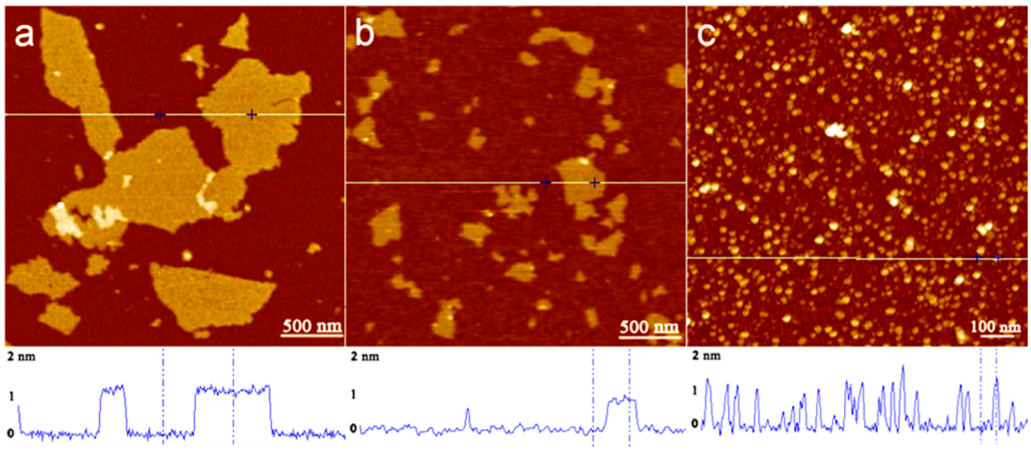

Figure 2. AFM images of GO1 (a), GO2 (b), and GO3 (c). The results demonstrated the different lateral nanometer sizes of GO1, GO2, and GO3.

nanometer sizes were different. GO1 possessed the largest nanometer size, which is above 500 nm. With an increasing time of oxidation, GO2 and GO3 possessed an average nanometer size of ~200 nm and ~40 nm, respectively. GOs with different nanometer sizes ensure that we can examine the nanometer size effect of GO on the interaction of GO with DNA, which has not yet been adequately examined.

Next, we investigated the nanometer size effect of GO on the DNA–GO interaction based on the fluorescence quenching ability of GO. We incubated the fluorophore (FAM (carboxyfluorescein))-modified DNA (FAM–DNA) with GO1 (0.5 μg/mL), GO2 (0.5 μg/mL), and GO3 (0.5 μg/mL). Then the fluorescence spectrum was collected. The free FAM–DNA demonstrated the highest fluorescent intensity (~280 au), and the mixture of FAM–DNA with GO demonstrated lower fluorescent intensity due to the fluorescence quenching ability of GO (Figure 3). Interestingly, we found that the quenching efficiency of GO1 (~48.8%) is ~3.6 times higher than that of GO3 (~13.4%). The higher quenching efficiency is probably originated from the relatively strong interaction between DNA and GO1.

To fully understand the nanometer size effect of GO on the GO–DNA interaction, we investigated the interaction between GO and FAM-modified DNAs with different lengths and compositions (for example, FAM-A10 represents FAM-modified DNA with 10 consecutive adenines). These DNAs include FAM-A10, FAM-A20, FAM-A40, FAM-C10, FAM-C20, FAM-C40, FAM-T10, FAM-T20, and FAM-T40. Due to the high fluorescence quenching ability of guanine, DNA with consecutive guanines was not employed. Then we incubated

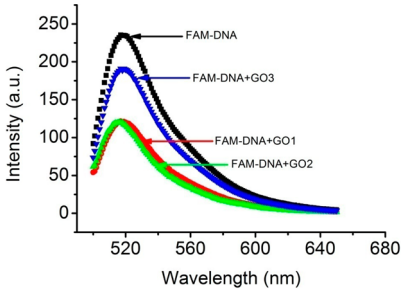

Figure 3. The fluorescence spectrum of FAM–DNA, the mixture of FAM–DNA and GO1, the mixture of FAM–DNA and GO2, and the mixture of FAM–DNA and GO3, demonstrating that GO1 and GO2 have quenching efficiency higher than that of GO3.

these DNAs with GO1, GO2, and GO3 in different concentrations (from 0.5 μg/mL to 10 μg/mL). After calculation of the quenching efficiency, we analyzed the DNA–GO interactions (Figure 4).

First, we investigated the interaction between GOs and DNAs with consecutive adenines (Figure 4, top). For different concentration of GOs, the quenching efficiency increased monotonically along with the increase of concentration of GOs. At a higher concentration of GO, the quenching efficiency reached nearly 100%. For different lateral nanometer sizes of GO, the quenching efficiency of GO2 was slightly higher than that of GO1 whereas GO3 possessed the lowest quenching efficiency. For different lengths of DNA, the quenching efficiency is inversely related to the length of DNA. For

dx.doi.org/10.1021/ac500627r | Anal. Chem. 2014, 86, 4047–4051

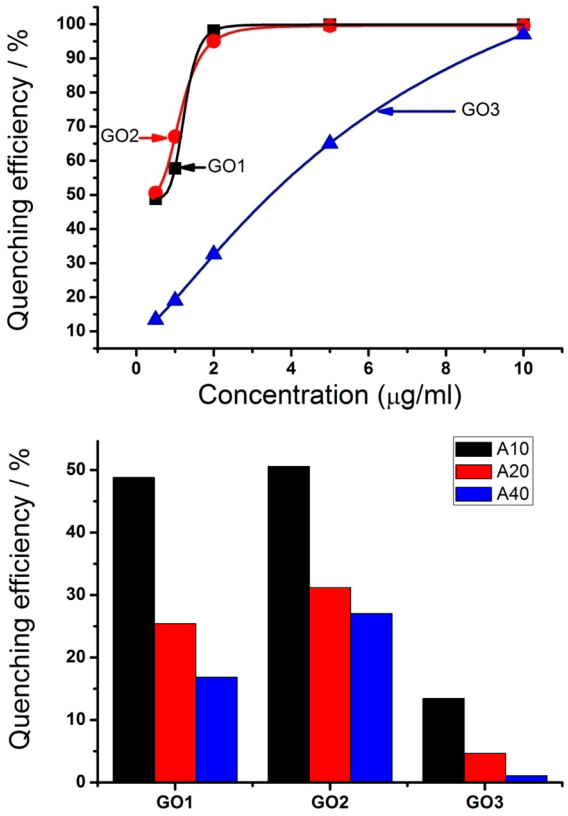

Figure 4. (Top) DNAs with consecutive adenines were employed to interact with GOs with different nanometer sizes and concentrations. (Bottom) The quenching efficiency is inversely related to the length of DNA.

example, the quenching efficiency of GO1 to FAM-A10 was ~48.8%. However, the quenching efficiency decreased to 16.8% when the length of DNA was increased to 40 bases (FAM-A40, Figure 4, bottom). Similar effects between GOs and DNAs with consecutive cytosines and thymines were obtained, respectively (Figures S1 and S2, Supporting Information).

The above investigation demonstrated that the GO−DNA interaction is nanometer size dependent. GO3 possessed the lowest fluorescence quenching efficiency, which indicated that the interaction between GO3 and DNA was weaker. As previously reported, even though both the GO and DNA are negatively charged, the DNA can still be adsorbed on the surface of GO.[24] The forces that drive the adsorption include $\pi-\pi$ stacking interaction and hydrophobic interaction.[24,34] The negative charges on the surface of GO contribute much less when the nanometer size is large (>200 nm). However, when the nanometer size of GO is decreased to 40 nm, the charge density increases because of the repeated oxidation, and the negative charges provide a reverse force that drives the DNA apart from GO, which leads to lower quenching efficiency. The sp^2 domains in the basal plane of GO and reduced GO provide the main driving force for the binding of DNA to GO and reduced GO.[24] The reduced GO may have similar size dependent effects.

The excellent differentiation ability of GO to single-stranded DNA and double-stranded (or folded) DNA is widely used to design various sensors for DNA/RNA, proteins, small molecules, and ions.[22−41] These sensors, characterized by high sensitivity, high specificity, and simple operation, have attracted extensive interest in recent years. However, the nanometer size effect of GO has not yet been adequately investigated and used to design sensors. Here, on the basis of the above nanometer size effects of GO on the GO−DNA interaction, we rationally designed sensors with tunable dynamic ranges (Figure 5 and Table 1). There are various realistic demands that require broad dynamic range such as viral load monitoring.[43] Likewise, some applications require high sensitivity (a steep relationship between target concentration and output signal) such as drug monitoring with narrow therapeutic range and logic gates.[44−47] As a test bed, we

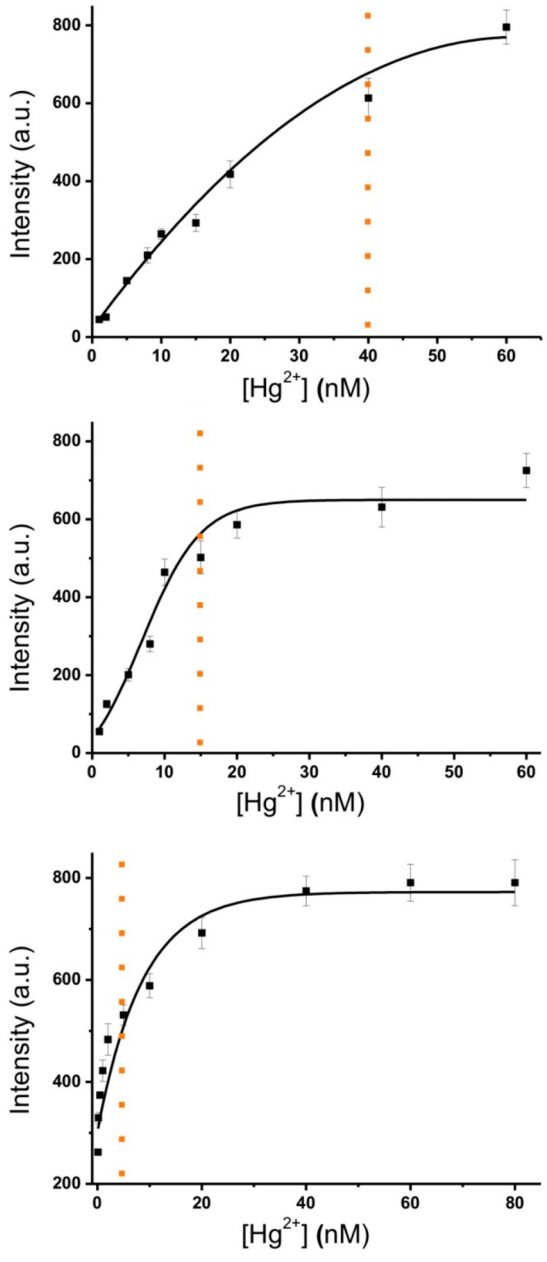

Figure 5. Titration curves of mercury sensors. By using different nanometer sizes of GO, the dynamic ranges of mercury sensors were programmed. (top) Sensor based on GO1 demonstrated broad dynamic range from 1 nM to 40 nM. (middle) Sensor based on GO2 demonstrated dynamic range from 1 nM to 15 nM. Sensor based on GO3 (bottom) demonstrated narrow dynamic range (0.1 nM to 5 nM) and high sensitivity. Dashed yellow lines indicate the limit of linearity (LOL) for each sensor.

dx.doi.org/10.1021/ac500627r | Anal. Chem. 2014, 86, 4047−4051

Table 1. Dynamic Ranges of Mercury Sensors by Using Different Lateral Nanometer Sizes of GO

GO type	sensitivity (slope of titration curve)/ nM^{-1}	limit of linearity (LOL)/nM	limit of detection (LOD)/nM	figure
GO1 (>500 nm)	15.3 ± 1.27	40	1	Figure 5, top
GO2 (~200 nm)	33.5 ± 2.79	15	1	Figure 5, middle
GO3 (~40 nm)	106.2 ± 3.96	5	0.1	Figure 5, bottom

employed a specific probe for mercury ions, which is a T-rich sequence, to build sensors for Hg^{2+} (for the detection of metal ions, some other research groups developed a very sensitive and specific detection platform based on some non-nucleic acid probes[48−50]). Here we are focusing on the interaction of GO and DNA; therefore, a DNA probe with a T-rich sequence was selected. Without Hg^{2+}, the probe is single stranded and can be easily adsorbed on the surface of GO. The fluorescence is quenched in this state. With Hg^{2+}, the probe folds into a secondary structure that cannot be adsorbed on the surface of GO. Then the fluorescence is liberated in this state. We programmed the dynamic ranges for Hg^{2+} detection by using the nanometer size effect of GO. At first, we employed GO1 and obtained a broad dynamic range (1 nM to 40 nM). Then we narrowed the dynamic range by using GO2 and GO3 (Figure 5 and Table 1). The sensitivity (slope of titration curve) was programmed, too. We obtained the highest sensitivity, 106.2 nM^{-1}, when we employed GO3. These programmed dynamic ranges and sensitivities originated from the different affinities between GO and single-stranded DNA. The affinity between GO with large lateral nanometer size (such as GO1 and GO2) and DNA is relatively strong; more Hg^{2+} is required to stabilize the folded structure to liberate the fluorescence.

CONCLUSION

GO is the most promising nanomaterial and is widely used in biosensors and bioimaging. However, the nanometer size effect of GO has not yet been adequately investigated. In summary, we have examined the nanometer size effect of GO on the DNA−GO interaction. We concluded that the interaction between GO and DNA is nanometer size dependent. GO with large size has relatively stronger quenching ability for fluorophore-modified DNAs. Our interesting findings were successfully employed to program the dynamic range and sensitivity of GO−DNA interaction-based ion biosensors.

EXPERIMENTAL DETAILS

Materials. DNA oligonucleotides were synthesized and purified by Jieli Biotechnology Co. (Shanghai, China). The sequences of oligonucleotides used are shown in Table 2. Graphite powder (<20 μm) was purchased from Sigma-Aldrich (Shanghai, China). All other chemicals were of analytical grade and purchased from China National Pharmaceutical Group Corporation (Shanghai, China) and used without purification. Water was purified using a Millipore filtration system (Millipore, Advantage A10).

Preparation and Characterization of Different Sized GO Nanosheets. Three different graphene oxide (GO) nanosheets were synthesized from graphite powder based on the modified Hummers method;[42] see the detailed process in our previous work.[51] A droplet of graphene oxide nanosheet dispersion was cast onto a fresh cleaved mica surface and dried at room temperature, and atomic force microscopy (AFM) images were recorded using a Nanoscope IIIa apparatus (Digital Instruments, Tonawanda, NY) at 25 °C and 30% humidity.

Fluorescence Assays. In the fluorescence quenching assays, FAM-labeled single-stranded DNA (with a final concentration of 20 nM) were incubated with different sized graphene oxide nanosheets of different concentrations (0.5 μg/mL, 1 μg/mL, 2 μg/mL, 5 μg/mL, and 10 μg/mL) in the PBS buffer (100 mM NaCl, 10 mM PB, 10 mM $MgCl_2$, pH 7.4), and the fluorescence was measured after 20 s by a Hitachi F-4500 fluorescence spectrophotometer with excitation at 494 nm and emission range from 505 to 650 nm.

In heavy metal ion (Hg^{2+}) assays, FAM-tagged mercury oligonucleotide (with a final concentration of 20 nM) was incubated with Hg^{2+} at a series of concentrations in MOPS (3-*N*-morpholinopropanesulfonic acid) buffer (10 mM with 50 mM $NaNO_3$, pH 7.2) for 5 min. Then GO solution with different final concentrations (2 μg/mL for GO1, 4 μg/mL for GO2, and 10 μg/mL for GO3) was added to this mixture, and fluorescence measurements were performed after 2 min.

ASSOCIATED CONTENT

Supporting Information

Supporting figures. This material is available free of charge via the Internet at http://pubs.acs.org.

AUTHOR INFORMATION

Corresponding Author

*Fax: 021-39194173. E-mail: huangqing@sinap.ac.cn.

Author Contributions

‖These authors contributed equally.

Table 2. DNA Sequences Employed in This Work

name	sequence (5′-3′)
A10	AAAAAAAAAA-FAM
T10	TTTTTTTTTT-FAM
C10	CCCCCCCCCC-FAM
A20	AAAAAAAAAAAAAAAAAAAA-FAM
T20	TTTTTTTTTTTTTTTTTTTT-FAM
C20	CCCCCCCCCCCCCCCCCCCC-FAM
A40	AAAAAAAAAAAAAAAAAAAAAAAAAAAAAAAAAAAAAAAA-FAM
T40	TTTTTTTTTTTTTTTTTTTTTTTTTTTTTTTTTTTTTTTT-FAM
C40	CCCCCCCCCCCCCCCCCCCCCCCCCCCCCCCCCCCCCCCC-FAM
probe for Hg^{2+}	FAM-TTCTTTCTTCCCCTTGTTTGTT

dx.doi.org/10.1021/ac500627r | *Anal. Chem.* 2014, 86, 4047−4051

Notes

The authors declare no competing financial interest.

■ ACKNOWLEDGMENTS

This work was supported by the National Natural Science Foundation of China (31371015, 31300825) and the Shanghai Municipal Commission for Science and Technology (13NM1402300).

■ REFERENCES

(1) Chauhan, V. P.; Stylianopoulos, T.; Martin, J. D.; Popovic, Z.; Chen, O.; Kamoun, W. S.; Bawendi, M. G.; Fukumura, D.; Jain, R. K. *Nat. Nanotechnol.* **2012**, *7*, 383.
(2) Chen, A. B. K.; Kim, S. G.; Wang, Y. D.; Tung, W. S.; Chen, I. W. *Nat Nanotechnol* **2011**, *6*, 237.
(3) Xu, Z.; Xiao, F. S.; Purnell, S. K.; Alexeev, O.; Kawi, S.; Deutsch, S. E.; Gates, B. C. *Nature* **1994**, *372*, 346.
(4) Gao, L. Z.; Zhuang, J.; Nie, L.; Zhang, J. B.; Zhang, Y.; Gu, N.; Wang, T. H.; Feng, J.; Yang, D. L.; Perrett, S.; Yan, X. *Nat. Nanotechnol.* **2007**, *2*, 577.
(5) Lei, Y.; Mehmood, F.; Lee, S.; Greeley, J.; Lee, B.; Seifert, S.; Winans, R. E.; Elam, J. W.; Meyer, R. J.; Redfern, P. C.; Teschner, D.; Schlogl, R.; Pellin, M. J.; Curtiss, L. A.; Vajda, S. *Science* **2010**, *328*, 224.
(6) Tisdale, W. A.; Williams, K. J.; Timp, B. A.; Norris, D. J.; Aydil, E. S.; Zhu, X. Y. *Science* **2010**, *328*, 1543.
(7) Campbell, C. T.; Parker, S. C.; Starr, D. E. *Science* **2002**, *298*, 811.
(8) Lauritsen, J. V.; Kibsgaard, J.; Helveg, S.; Topsoe, H.; Clausen, B. S.; Laegsgaard, E.; Besenbacher, F. *Nat. Nanotechnol.* **2007**, *2*, 53.
(9) Kan, S.; Mokari, T.; Rothenberg, E.; Banin, U. *Nat. Mater.* **2003**, *2*, 155.
(10) Choi, H.; Ko, J. H.; Kim, Y. H.; Jeong, S. *J. Am. Chem. Soc.* **2013**, *135*, 5278.
(11) Li, Q. Q.; Zhang, S.; Dai, L. M.; Li, L. S. *J. Am. Chem. Soc.* **2012**, *134*, 18932.
(12) Norberg, N. S.; Arthur, T. S.; Fredrick, S. J.; Prieto, A. L. *J. Am. Chem. Soc.* **2011**, *133*, 10679.
(13) Fan, K. L.; Cao, C. Q.; Pan, Y. X.; Lu, D.; Yang, D. L.; Feng, J.; Song, L. N.; Liang, M. M.; Yan, X. Y. *Nat. Nanotechnol.* **2012**, *7*, 459.
(14) Jiang, W.; Kim, B. Y. S.; Rutka, J. T.; Chan, W. C. W. *Nat. Nanotechnol.* **2008**, *3*, 145.
(15) Jun, Y. W.; Huh, Y. M.; Choi, J. S.; Lee, J. H.; Song, H. T.; Kim, S.; Yoon, S.; Kim, K. S.; Shin, J. S.; Suh, J. S.; Cheon, J. *J. Am. Chem. Soc.* **2005**, *127*, 5732.
(16) Yang, K.; Wan, J. M.; Zhang, S.; Tian, B.; Zhang, Y. J.; Liu, Z. *Biomaterials* **2012**, *33*, 2206.
(17) Zhu, C. F.; Zeng, Z. Y.; Li, H.; Li, F.; Fan, C. H.; Zhang, H. *J. Am. Chem. Soc.* **2013**, *135*, 5998.
(18) Liu, X. Q.; Wang, F.; Aizen, R.; Yehezkeli, O.; Willner, I. *J. Am. Chem. Soc.* **2013**, *135*, 11832.
(19) Song, Y. J.; Qu, K. G.; Zhao, C.; Ren, J. S.; Qu, X. G. *Adv. Mater.* **2010**, *22*, 2206.
(20) Dikin, D. A.; Stankovich, S.; Zimney, E. J.; Piner, R. D.; Dommett, G. H. B.; Evmenenko, G.; Nguyen, S. T.; Ruoff, R. S. *Nature* **2007**, *448*, 457.
(21) Zhu, Y. W.; Murali, S.; Cai, W. W.; Li, X. S.; Suk, J. W.; Potts, J. R.; Ruoff, R. S. *Adv. Mater.* **2010**, *22*, 3906.
(22) Lee, J.; Kim, Y. K.; Min, D. H. *Anal. Chem.* **2011**, *83*, 8906.
(23) Zhou, J.; Xu, X. H.; Liu, W.; Liu, X.; Nie, Z.; Qing, M.; Nie, L. H.; Yao, S. Z. *Anal. Chem.* **2013**, *85*, 5746.
(24) He, S. J.; Song, B.; Li, D.; Zhu, C. F.; Qi, W. P.; Wen, Y. Q.; Wang, L. H.; Song, S. P.; Fang, H. P.; Fan, C. H. *Adv. Funct. Mater.* **2010**, *20*, 453.
(25) Zuo, X. L.; He, S. J.; Li, D.; Peng, C.; Huang, Q.; Song, S. P.; Fan, C. H. *Langmuir* **2010**, *26*, 1936.
(26) Wen, Y. Q.; Xing, F. F.; He, S. J.; Song, S. P.; Wang, L. H.; Long, Y. T.; Li, D.; Fan, C. H. *Chem. Commun.* **2010**, *46*, 2596.
(27) Wen, Y. Q.; Peng, C.; Li, D.; Zhuo, L.; He, S. J.; Wang, L. H.; Huang, Q.; Xu, Q. H.; Fan, C. H. *Chem. Commun.* **2011**, *47*, 6278.
(28) He, S. J.; Liu, K. K.; Su, S.; Yan, J.; Mao, X. H.; Wang, D. F.; He, Y.; Li, L. J.; Song, S. P.; Fan, C. H. *Anal. Chem.* **2012**, *84*, 4622.
(29) Li, Y. H.; Duan, Y.; Zheng, J.; Li, J. S.; Zhao, W. J.; Yang, S.; Yang, R. H. *Anal. Chem.* **2013**, *85*, 11456.
(30) Cai, L. P.; Zhan, R. Y.; Pu, K. Y.; Qi, X. Y.; Zhang, H.; Huang, W.; Liu, B. *Anal. Chem.* **2011**, *83*, 7849.
(31) Tu, Y. Q.; Li, W.; Wu, P.; Zhang, H.; Cai, C. X. *Anal. Chem.* **2013**, *85*, 2536.
(32) Dong, H. F.; Zhang, J.; Ju, H. X.; Lu, H. T.; Wang, S. Y.; Jin, S.; Hao, K. H.; Du, H. W.; Zhang, X. J. *Anal. Chem.* **2012**, *84*, 4587.
(33) Lu, C. H.; Li, J.; Zhang, X. L.; Zheng, A. X.; Yang, H. H.; Chen, X.; Chen, G. N. *Anal. Chem.* **2011**, *83*, 7276.
(34) Liu, B. W.; Sun, Z. Y.; Zhang, X.; Liu, J. W. *Anal. Chem.* **2013**, *85*, 7987.
(35) Huang, P. J. J.; Liu, J. W. *Anal. Chem.* **2012**, *84*, 4192.
(36) Liu, S. J.; Wen, Q.; Tang, L. J.; Jiang, J. H. *Anal. Chem.* **2012**, *84*, 5944.
(37) Feng, B. Y.; Guo, L. J.; Wang, L. H.; Li, F.; Lu, J. X.; Gao, J. M.; Fan, C. H.; Huang, Q. *Anal. Chem.* **2013**, *85*, 7732.
(38) Lin, L.; Liu, Y.; Zhao, X.; Li, J. H. *Anal. Chem.* **2011**, *83*, 8396.
(39) Cui, L.; Chen, Z. R.; Zhu, Z.; Lin, X. Y.; Chen, X.; Yang, C. J. *Anal. Chem.* **2013**, *85*, 2269.
(40) Ocsoy, I.; Paret, M. L.; Ocsoy, M. A.; Kunwar, S.; Chen, T.; You, M. X.; Tan, W. H. *ACS Nano* **2013**, *7*, 8972.
(41) Ocsoy, I.; Gulbakan, B.; Chen, T.; Zhu, G. Z.; Chen, Z.; Sari, M. M.; Peng, L.; Xiong, X. L.; Fang, X. H.; Tan, W. H. *Adv. Mater.* **2013**, *25*, 2319.
(42) Hummers, W. S.; Offeman, R. E. *J. Am. Chem. Soc.* **1958**, *80*, 1339.
(43) Vallee-Belisle, A.; Ricci, F.; Plaxco, K. W. *J. Am. Chem. Soc.* **2012**, *134*, 2876.
(44) Porchetta, A.; Vallee-Belisle, A.; Plaxco, K. W.; Ricci, F. *J. Am. Chem. Soc.* **2012**, *134*, 20601.
(45) Porchetta, A.; Vallee-Belisle, A.; Plaxco, K. W.; Ricci, F. *J. Am. Chem. Soc.* **2013**, *135*, 13238.
(46) Xiang, Y.; Wang, Z. D.; Xing, H.; Wong, N. Y.; Lu, Y. *Anal. Chem.* **2010**, *82*, 4122.
(47) Kang, D.; Vallee-Belisle, A.; Porchetta, A.; Plaxco, K. W.; Ricci, F. *Angew. Chem., Int. Ed.* **2012**, *51*, 6717.
(48) Li, Y.; Shi, L.; Qin, L.; Qu, L.; Jing, C.; Lan, M.; James, T. D.; Long, Y. *Chem. Commun.* **2011**, *47*, 4361.
(49) Li, Y.; Xu, D.; Long, Y. *Anal. Chim. Acta* **2011**, *701*, 157.
(50) Shi, L.; Song, W.; Li, Y.; Li, D.; Swanick, K. N.; Ding, Z.; Long, Y. *Talanta* **2011**, *84*, 900.
(51) Zhang, H.; Peng, C.; Yang, J. Z.; Lv, M.; Liu, R.; He, D. N.; Fan, C. H.; Huang, Q. *ACS Appl. Mater. Interfaces* **2013**, *5*, 1761.